Drug Development and Industrial Pharmacy, 2010; 36(10): 1225–1234

informa
healthcare

ORIGINAL ARTICLE

Preparation, characterization, pharmacokinetics, and tissue distribution of curcumin nanosuspension with TPGS as stabilizer

Yan Gao[1], Zhonggang Li[2], Min Sun[1], Houli Li[3], Chenyu Guo[1], Jing Cui[4], Aiguo Li[1], Fengliang Cao[1], Yanwei Xi[1], Hongxiang Lou[5] and Guangxi Zhai[1]

[1]Department of Pharmaceutics, College of Pharmacy, Shandong University, Jinan, China, [2]Center for New Drugs Evaluation, Shandong University, Jinan, China, [3]Division of Pharmaceutics, College of Pharmacy, The University of Texas at Austin, Austin, TX, USA, [4]Department of Pharmacy, Qilu Hospital of Shandong University, Jinan, China and [5]Department of Natural Product Chemistry, College of Pharmacy, Shandong University, Jinan, China

Abstract

Background: CUR is a promising drug candidate based on its good bioactivity, but use of CUR is potentially restricted because of its poor solubility and bioavailability. *Aim*: The aim of this study was to prepare an aqueous formulation of curcumin nanosuspension (CUR-NS) to improve its solubility and change its in vivo behavior. *Methods*: CUR-NS was prepared by high-pressure homogenization method. Drug state in CUR-NS was evaluated by powder X-ray diffraction. Pharmacokinetics and biodistribution of CUR-NS after intravenous administration in rabbits and mice were studied. *Results*: The solubility and dissolution of CUR in the form of CUR-NS were significantly higher than those of crude CUR. X-ray crystallography diffraction indicated that the crystalline state of CUR in nanosuspension was preserved. Pharmacokinetics and biodistribution results of CUR-NS after intravenous administration in rabbits and mice showed that CUR-NS presented a markedly different pharmacokinetic property as compared to the CUR solution. $AUC_{0-\infty}$ of CUR-NS (700.43 ± 281.53 μg/mL, min) in plasma was approximately 3.8-fold greater than CUR solution (145.42 ± 9.29 μg/mL min), and the mean residence time (194.57 ± 32.18 versus 15.88 ± 3.56 minutes) was 11.2-fold longer. *Conclusion*: Nanosuspension could serve as a promising intravenous drug-delivery system for curcumin.

Key words: *Curcumin; high-pressure homogenization; nanosuspensions; pharmacokinetics; tissue distribution*

Introduction

Despite recent development of new drugs in cancer treatment, severe adverse reactions continue to be a clinically important problem in cancer chemotherapy. The rapid termination of treatment using doxorubicin and cisplatin, and the like severely limits tumor eradication due to nephrotoxicity and cardiac toxicity[1,2]. Expected toxic effects from marketed drugs, even when used appropriately, are estimated to rank among the top 10 causes of death in the United States and to cost more than $30 billion annually. Besides, five pharmaceuticals have been reported to be removed from the market due to unexpected adverse events in 1 year[3]. All of these result in a need to develop low toxicity and cheap chemotherapy drugs. Curcumin [1,7-bis(4-hydroxy-3-methoxyphenyl)-1,6-heptadiene-3,5-dione, CUR] (Figure 1A), a natural compound isolated from the root of *Curcuma longa L.* (Zingiberaceae family) *rhizomes*, has a bright future in this field. It was found to have good bioactivity against cancers while having no toxic effects on normal cells as high as 50 μM[4]. Curcumin has been listed as the third generation of cancer chemopreventive drugs by the National Cancer Institution (NCI), National Institute of Health (NIH) of the United States since 2000 as an effective antimutagen

Address for correspondence: Prof./Dr. Guangxi Zhai, PhD, Department of Pharmaceutics, College of Pharmacy, Shandong University, 44 Wenhua Xilu, Jinan 250012, China. Tel: +86 531 88382015. E-mail: professorgxizhai@yahoo.cn

Yan Gao and Zhonggang Li contributed equally to the work

(Received 30 Jan 2010; accepted 11 Feb 2010)

ISSN 0363-9045 print/ISSN 1520-5762 online © Informa UK, Ltd.
DOI: 10.3109/03639041003695139

and anticancer-promoting agent. Many clinical studies have been undergoing or completed in treatment of multiple myeloma, rheumatoid arthritis, rectal, advanced pancreatic, and metastatic colon cancers[5]. Additionally, the egligible cost of CUR has also rendered curcumin an attractive molecule to explore further[4,6,7].

Although CUR is a promising drug candidate, use of CUR is potentially restricted because of its poor solubility. It is reported that the solubility of CUR in plain aqueous buffer (pH 5.0) is 11 ng/mL[8], which indicates that it is impossible to prepare an aqueous solution formulation of curcumin for intravenous use[9]. Additionally, the oral absorption of CUR in humans is also very poor[10]. In order to enhance the solubility of CUR and improve the use in clinic, a suitable vehicle or dosage form is needed.

Nanocrystal suspension, nanosuspension for short, is a carrier-free nanoparticle system containing only pure drug crystals and minimum surfactant and/or polymer for stabilization[11,12]. There is a great increase in the drug solubility and dissolution velocity for the poorly soluble drugs in the form of nanosuspension[13–15]. Moreover, nanosuspension can protect the entrapped drugs from degradation, hydrolysis, and oxidation, can target infection sites or organs via phagocytosis effect to the reticuloendothelial system (RES), can prolong the circulation time and reduce the toxicity and adverse effects caused by some surfactants, organic solvents, or polymers[16,17]. Nowadays, aqueous nanocrystal suspension is a prevalent dosage form with many drugs available on the market such as fenofibrate, rapamune, and emend[18]. However, curcumin loaded nanosuspension has not been reported.

TPGS (D-α-tocopheryl polyethylene glycol 1000 succinate, Figure 1B) is a water-soluble derivative of the natural Vitamin E (α-tocopherol) and consists of a hydrophilic polar head portion of polyethylene glycol 1000. It is reported that TPGS can present good emulsification effect, excellent drug stabilization, and solubilization[19–21]. Enhanced therapeutic effect is also obtained in the nanoparticle formulation of high hydrophobic anticancer drugs using TPGS as the stabilizer[18,22–24]. Meanwhile, TPGS has been demonstrated to be an effective P-glycoprotein (P-gp) inhibitor. Coadministration of TPGS and anticancer drugs may effectively transport the drug into the P-gp-mediated multidrug resistant (MDR) cancer cells[25–29]. The advantages of TPGS have rendered it attractive for further exploitation in nanosuspension.

In this study, TPGS-stabilized CUR-NS, a new nanosized formulation with high drug loading for intravenous (i.v.) administration of CUR, was prepared by high-pressure homogenization. The physicochemical characteristics including solubility, dissolution, drug-existing state, particle size, morphology, and zeta potential of CUR-NS were evaluated. The pharmacokinetics in rabbits and biodistribution in mice of CUR-NS by i.v. administration were also studied.

Materials and methods

Materials

Curcumin was purchased from BASF, Germany. PEG 400 was obtained from Shanghai Chemical Reagent Co., Ltd. (Shanghai, China). TPGS was procured from Sigma-Aldrich Chemical Co. (St. Louis, MO, USA). Mannitol was purchased from Sinopharm Chemical Reagent Co. Ltd., China. Acetonitrile of high performance liquid chromatography (HPLC) grade was purchased from Tianjin SiYou chemical agent Co., Ltd. (Tianjin, China). Other chemicals and solvents were of analytical reagent grade.

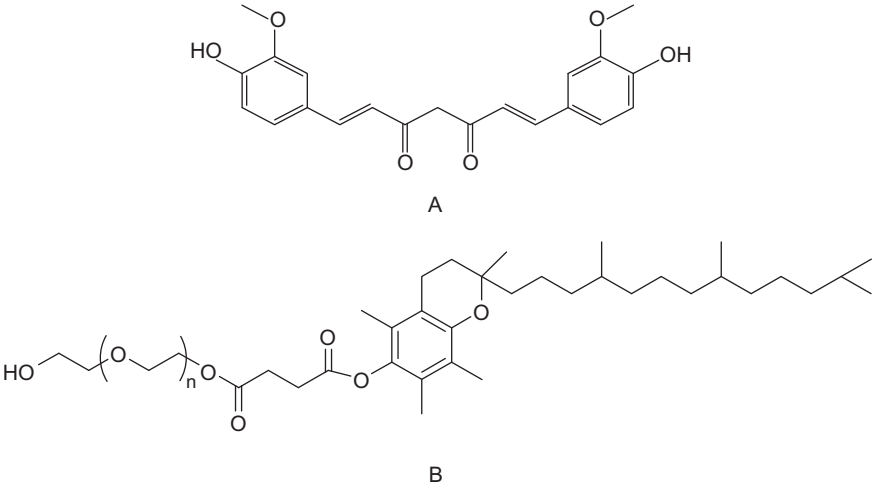

Figure 1. Chemical structures of curcumin (A) and TPGS (B).

Formulations

CUR-NS, consisting of 1.0 g of CUR, 1.0% (w/v) of TPGS and 98.3% (w/v) of demineralized water, was prepared by trituration first, followed by ultra-turrax homogenization and high-pressure homogenization[15,30]. Briefly, pristine CUR was dispersed in an aqueous surfactant solution containing appropriate amounts of TPGS under triturating. Then the dispersion was further premixed using a Heidolph homogenizer (DIAX 900; Heidolph Elektro, Kelheim, Germany) at 26,000 rpm for 3 minutes. The obtained mixture was homogenized using a Niro-Soavi high-pressure homogenizer (NS1001L; ATS Co. Ltd., Parma, Italy) with the process as follows: 200 bar with 2 cycles and 500 bar with 5 cycles, then 1500 bar with 20 cycles. The resultant suspension was subjected to centrifugation at 1000 rpm for 5 minutes to exclude all particles larger than 5 μm with microscope (YS-2; Nikon Co., Tokyo, Japan) observation for assurance. All operations were carried out using a cooling device to maintain sample temperature at a low temperature.

To improve the stability of the delivery and to further study the physical state of drug in the formulation, the resulting nanosuspension added with 5% (w/v) of mannitol as a cryoprotectant was pre-frozen using an ultra-low temperature refrigerator (DW-HL218; Chinateah Meiling) at –80°C for 24 hours, then the resultant solids were freeze-dried using a lyophilizer (FD5-series; SIM, Los Angeles, CA, USA). The dry powder was stored at room temperature and was reconstituted to nanosuspension by addition of distilled water and sonication before application.

As control, CUR solution was prepared according to the previous report[31]. 40 mg of CUR was dissolved in 1.5 mL of dimethyl acetamide and 4.5 mL of PEG 400, and the obtained solution was diluted to 10 mL with isotonic dextrose solution.

As CUR was a highly photolabile compound, all operations were performed under subdued light.

Characterization

Morphology

The morphological evaluation of freshly prepared and reconstituted nanosuspension from CUR-NS dry powder was conducted using a transmission electron microscopy (TEM, JEM-1200EX; JEOL, Tokyo, Japan). After dilution with distilled water, the samples were negatively stained with 2% (w/v) phosphotungstic acid for TEM observation.

Particle size and zeta potential

Particle size analysis of CUR-NS was performed by photon correlation spectroscopy (PCS) using a particle sizer (Zetasizer 3000 HAS; Malvern Instruments Ltd., Malvern, Worcestershire, UK) at a fixed angle of 90° at 25°C. The measurement was conducted using a He-Ne laser of 633 nm and the particle size analysis data were evaluated using the volume distribution from Gaussian distribution. Zeta potential was analyzed by TV microscopic Electrophoresis System (DXD-II; Optics Co., Ltd., Suzhou, China) at 25°C after dilution with distilled water.

Powder X-ray diffraction

The crystalline state of drug in nanosuspension was estimated by an X-ray diffractometer (D/max r-B; Rigaku Co., Tokyo, Japan). Diffraction of each sample was researched with a Cu line as the source of radiation. Standard runs using a 40 kV voltage, a 40 mA current, and a scanning rate of 2°/min over a 2θ range of 6–40° were performed. Powder X-ray diffraction (PXRD) patterns were determined for buck CUR, TPGS, physical mixture of CUR and TPGS (PM), and CUR-NS powder.

Solubility measurement

Equilibrium solubility of CUR-NS or physical mixture (PM) was determined by shake-flask method[32,33]. Excess amount of buck CUR, CUR-NS, and PM were added in water and equilibrated in shaker water bath (HZ-92 1K; Taicang Instrument Ltd., Taicang, China) at 37°C for 48 hours, respectively. Vials were sealed to avoid changes due to evaporation and shielded from light to prevent any degradation of CUR. After the equilibrium was reached, suspensions were first subjected to ultracentrifuge to discard the undissolved drug particles and then filtered through 0.22 μm syringe filters. An aliquot of filtrate was assayed by HPLC to evaluate the dissolved amount of CUR.

Dissolution evaluation

In vitro dissolution behavior study was carried out following Chinese Pharmacopoeia specifications for poorly soluble drugs using a dissolution apparatus (RC-3B; Tianguang Optical Instrument Co. Ltd., Tianjin, China) with the paddle method. In order to ensure sink conditions, PBS (0.01 M, pH 7.4) containing 2% of sodium dodecyl sulfate (SDS) was selected as dissolution medium. Briefly, the samples containing equivalent of CUR (10 mg) were dropped into 900 mL dissolution medium and incubated at 37 ± 0.5°C at 75 rpm. Samples (5 mL) were collected at predetermined time intervals (2, 5, 10, 20, 30, 40, 50, 60, 75, 90, 120 minutes), then filtered through a 0.22 μm syringe filters, and equal blank medium at 37°C was compensated immediately after the withdrawal to sustain the sink condition. The dissolved CUR in the sample solution was determined spectrophotometrically with wavelength at 425 nm.

Stability study

Storage stability was studied by storing CUR-NS powder at 4°C for up to 3 months. Periodically, samples were withdrawn and the particle size as well as CUR content was measured.

In vivo studies on pharmacokinetics and biodistribution

Animals

New Zealand white rabbits (weighing 2.5 ± 0.2 kg) and Kunming mice (weighing 20 ± 5 g), supplied by the Experimental Animal Center of Shandong University (Jinan, China), were used for pharmacokinetic and biodistribution studies. At first, the animals were acclimatized in metabolic cages at a temperature of 25 ± 2°C and a relative humidity of 40–70% under natural light/dark conditions for at least 7 days with water and a solid diet freely available before dosing. Prior to the experiment the animals were kept under fasting overnight. All experimental procedures abided by the ethics and regulations of animal experiments of Pharmaceutical Sciences, Shandong University, China (Jinan, China).

Pharmacokinetics study

Eight rabbits divided into two groups were used for pharmacokinetics study. CUR solution and CUR-NS were given as a single bolus with a dose of CUR at 15 mg/kg. At predetermined time points (5, 10, 20, 30 minutes, 1, 1.5, 2, 3, 5, 8, and 12 hours), 1 mL of blood sample was collected from rabbits via marginal ear vein into heparinized tubes. The samples were centrifuged at 3000 rpm for 15 minutes immediately for isolation of the plasma. Samples were stored at −20°C until further analysis.

Tissue distribution study

The in vivo tissue distribution studies of CUR-NS were carried out in Kunming mice. Mice were randomly assigned to two groups with four mice at each time points. Two formulations, CUR-NS and CUR solution, were injected to mice via caudal vein [dilating with 75% (v/v) of ethanol solution] with a dose of CUR equivalent to 20 mg/kg, respectively. Mice were sacrificed by carbon dioxide asphyxiation at 0.167, 0.25, 1, or 3 hours time points post-dosing and brain, heart, lung, liver, spleen, and kidney were harvested. All of the samples were stored at −20°C until analysis.

High performance liquid chromatography analysis

The homogenized samples were prepared by adding 1 mL of physiological saline to each of the precisely weighed tissue (lower than 0.5 g) and homogenized. To 500 μL of tissue homogenate or plasma sample, 100 μL of citric buffer (pH 4) was added and votexed for 30 seconds, and then the resultant mixture samples were extracted with 2 mL acetic ether twice by vortexing vigorously for 3 minutes. Each sample was then centrifuged at 3500 rpm for 5 minutes at 4°C. The supernatant was transferred to a clean 1.5 mL micro-centrifuge tube and dried under a steam of nitrogen gas. Each sample was reconstituted with 100 μL of methanol and centrfugated at 10,000 rpm for 10 minutes to discard the undissolved impurity. Twenty μL of supernatant was injected into HPLC for analysis.

CUR in the samples was determined by HPLC analysis using a LC-10 ATvp pump, a SPD-10Avp UV-vis detector (Shimadzu Co., Tokyo, Japan) with a 250 mm × 4.6 mm reverse phase stainless steel column packed with 5 μm particles (Elite Analytical Instrument Co. Ltd., Dalian, China). The mobile phase consisted of 1% (w/v) of citric acid solution, adjusted to pH 3.0 using a 1 M sodium hydroxide solution, and acetonitrile at the ratio of 58:42 (v/v) at a flow rate of 1 mL/min and the effluent was monitored at 425 nm. Pharmacokinetic parameters were evaluated using practical pharmacokinetic program version DAS 1.0[34].

Statistical analysis

Statistical data were analyzed using the Student's *t*-test with $P < 0.05$ as the minimal level of significance.

Results and discussion

Screening of the parameters of preparation technology

As shown in Figure 2, particle sizes of CUR-NS were becoming smaller and smaller with increased pressure and number of cycles. The ultra-turrax particles were mainly distributed in the range of 10–20 μm. When it was subjected to pressure of 500 bar, the amount of larger particles was reduced obviously and the partition of smaller particles increased simultaneously, which led to the decrease of the mean particle size. Moving on for another cycle or increasing pressure ended up with desired and homogenous nanosuspension. When a certain minimum value of particle size was achieved under a certain pressure, more homogenisation cycles couldn't lead to a continual reduction of particle size unless higher pressure was applied, but more cycles of run favored decreasing the width of size distribution and the incidence of Ostwald ripening by eliminating remaining large crystals[12,35]. As can be seen from Figure 2, when the pressure attained 1500 bar, particle size decreased significantly, and the treatment of 20 cycles resulted in more uniform distribution of particle size compared to that of 15 cycles. Therefore, the optimized procedure of CUR-NS should include the run of high pressure at 1500 bar for 20 cycles.

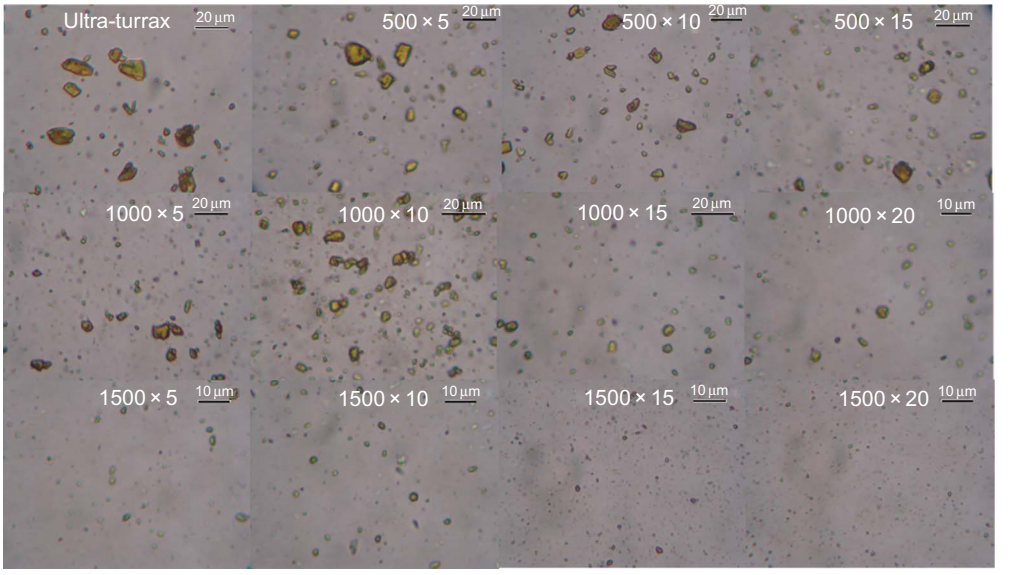

Figure 2. Light photograph of particles undergone different operations, pressure and cycles (bar × cycles).

The characterization of CUR-NS

Morphology

As shown in Figure 3, the particle in CUR-NS presented smaller and sphere-like shape under TEM, and there was no significant change in size after redispersion of the lyophilized powder in deionized water (Figure 3A) compared to that of freshly prepared samples (Figure 3B) without the treatment of lyophilization.

Particle distribution and zeta potential

Particle size of reconstituted nanosuspension from dried CUR-NS powder was determined by photon correlation spectroscopy (PCS). As shown in Figure 4, the nanoparticles in the suspension presented a relative narrow size distribution with the mean particle size of about 210.2 nm and *PI* value of 0.123.

It was reported that the particles in the dispersed systems tended to grow due to the Gibbs–Thomson effect, which is a result of the differences in solubility between small and large particles in suspension[35,36]. The phenomenon is called Ostwald ripening. It could be explained by Ostwald–Freundlich's equation below:

$$\ln \frac{S}{S_0} = \frac{2M\gamma}{\rho r \mathrm{RT}}, \quad (1)$$

where S is the solubility, S_0 is the solubility of a flat sheet ($r = \infty$), M is the molecular weight of the solid, γ is the interfacial tension, R is the gas constant, T is the absolute temperature, r is the radius, and ρ is the density of the solid.

As can be seen from the Ostwald–Freundlich's equation, the solubility of a certain material is inversely

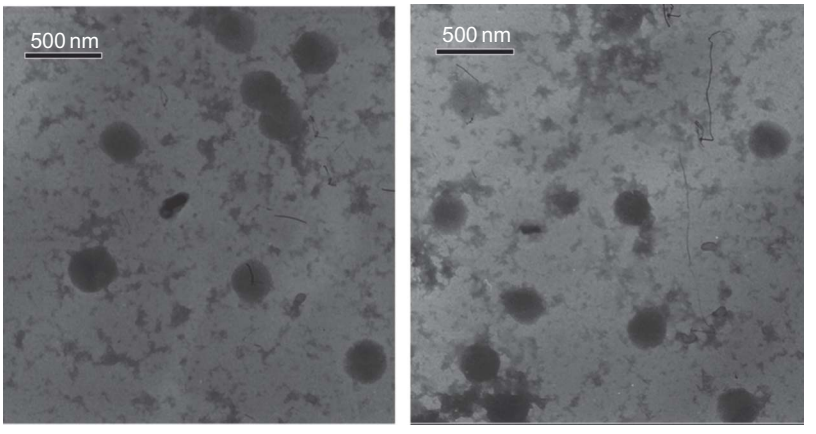

Figure 3. TEM photograph of CUR-NS before (A) and after the lyophilization (B).

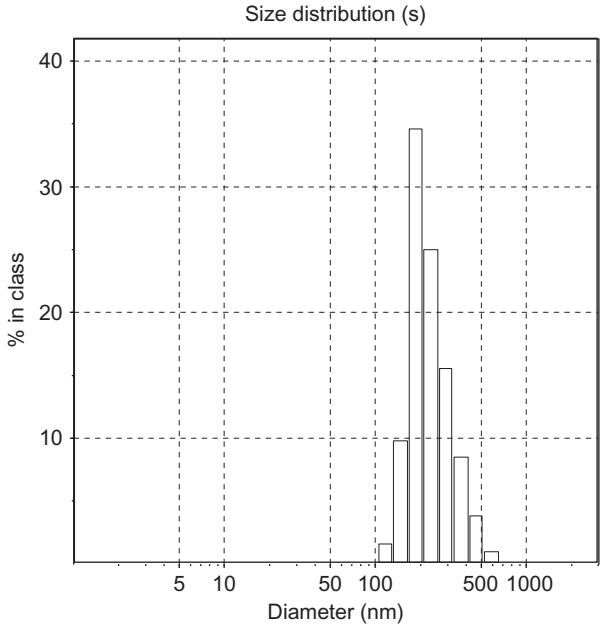

Figure 4. The size distribution of the CUR-NS.

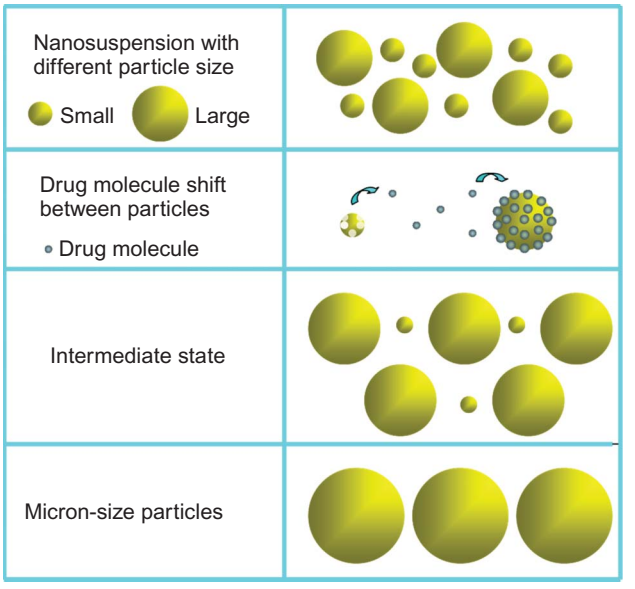

Figure 5. Schematic representation of Ostwald ripening to CUR-NS (Not to scale).

correlated to the material's size. Based on the principle, the instability of nanoparticles in the nanosuspension system can be illustrated in Figure 5. As the particle size decreases, the solubility increases. Therefore, in a nano-sized dispersed system, the higher solubility of small particles and the lower solubility of large particles resulted in a concentration gradient between them. The dissolved molecules in the vicinity of the smaller particles could easily diffuse from the high concentration to the low concentration and sediment on the surface of the large particles. The continual diffusion leads to complete dissolution of the small particles until they totally disappear while the large particles grow up into microsized particles[37]. Therefore, lyophilization was needed to avoid Ostwald ripening and to obtain a more stable nanosuspension. Lyophilization was performed with 5% mannitol as a cryoprotectant.

Moreover, the zeta potential has an important effect on the storage stability of colloid dispersion system. It reflects the electric barriers preventing the nanoparticles from aggregation and agglomeration. Particle aggregation is likely to occur if particles possess too low a zeta potential to provide sufficient electric repulsion or steric barriers between each other. As a rule of thumb, a zeta potential of at least −30 mV for electrostatically or −20 mV for sterically stabilized systems is desired to obtain a physically stable nanosuspension. About 20 mV can provide only a short-term time stability; zeta potential in the range −5 to 5 mV indicates fast aggregation[36]. Therefore, measurement of the zeta potential in certain cases allows predictions about the storage condition and suggests disposal time of nanosuspension. However, it is usually valid for nanosuspension system with low molecular weight stabilizers and pure electric stabilization. It would not be the case for nanoparticles containing some stabilizers with relatively higher molecular weight. As shown in Figure 6, each particle dispersed in the system is surrounded by oppositely charged ions that constituted the stern layer. Outside the stern layer, there are various compositions of hydrated counter-ion, forming a cloud-like area. This area is called the diffuse electric layer. Shear plane is a conceptual layer at the outmost part of this area. Theoretically, zeta potential is considered to be the electric potential at shear plane. The stern layer and part of the diffuse layer form the electric double layer, which plays an important role in the stability of the system. However, the large molecules or special polymers tend to extend to a very wide region with different length of tails. Short tails may be enclosed in the interior core in existence of counter-ion adsorbed around, which may lead to a reduction of the measured zeta potential in the stern plane. In the present study, TPGS stabilized CUR-NS systems were relatively stable even though the measured zeta potential was low (−14.84 ± 1.68 mV, $n = 3$), so it was speculated that thick layer of stabilizers had an overwhelming effect on stabilization in the TPGS system, where potential values of lower than 20 mV could also provide sufficient stabilization[38]. The result was consistent with the previous reports for nanosuspension systems including rilpivirine, itraconazole and fenofibrate with TPGS as stabilizer[18,39,40].

Crystalline state evaluation

The crystalline state of the samples was evaluated to prove the effect of high pressure homogenization treatment on

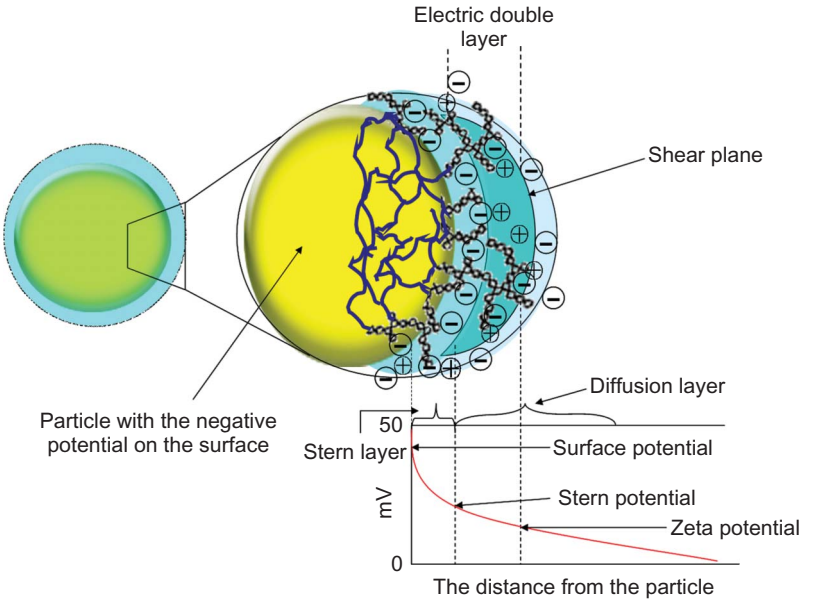

Figure 6. Structure of the TPGS-stabilized CUR-NS and schematic representation of the reduction of the measured zeta potential in the stern plane.

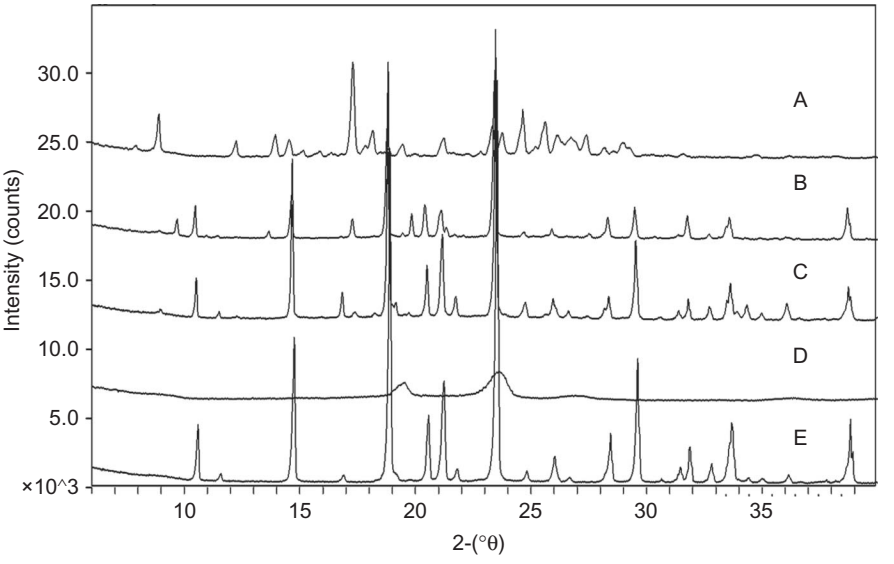

Figure 7. PXRD diffractograms of pristine CUR (A), TPGS stabilized CUR-NS (B), physical mixture of CUR, mannitol and TPGS (C), TPGS (D), mannitol (E).

the physical state of CUR. The PXRD patterns for pristine CUR, physical mixture (PM), and CUR-NS are displayed in Figure 7. Upon X-ray examinations, the pristine CUR, CUR-NS, and PM manifested specific peaks for CUR at the 2-(°θ) of 17°, which suggested that the crystallinity diffraction peaks of CUR was preserved in the CUR-NS formulation, indicating that the crystalline state of CUR was unaltered following the homogenization.

Solubility and dissolution velocity studies

The solubility of CUR was reported to be 11 ng/mL, negligible and far below the detection limit, in plain aqueous buffer (pH 5.0)[8], which makes it difficult to develop intravenous drug delivery for CUR. Nanosuspension, featured by the enhanced solubility for poor-soluble drug, could solve the problem effectively. CUR-NS showed enhanced solubility (9.45 ± 0.33 mg/L), which

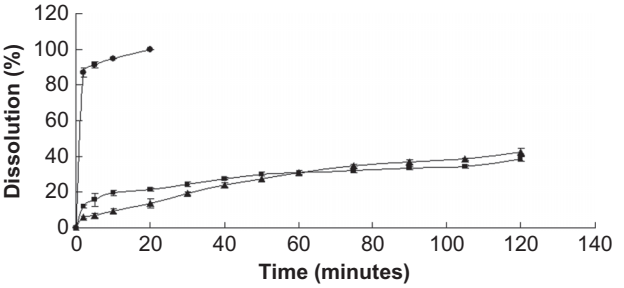

Figure 8. Dissolution curve of the CUR-NS (●), pristine CUR (■) and the PM of CUR and excipients (▲).

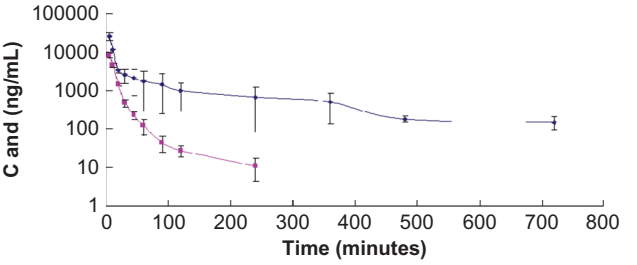

Figure 9. Mean CUR concentration-time profiles in plasma after intravenous administration of CUR solution (■) and CUR-NS (◆) to rabbits with dose 15 mg/kg (Data were given as mean ± SD, $n = 3$).

may be attributed to the nano-sized CUR particles and the solubilization effect of TPGS.

As shown in Figure 8, pristine CUR with microsize level, the mixture of pristine CUR and excipients, and dried CUR-NS powder presented obviously different dissolution behaviors in PBS (0.01 M, pH 7.4) containing 2% (w/v) of SDS as the dissolution medium to ensure sink conditions. Within 2 minutes almost 86.9% of CUR was dissolved from the dried nanocrystal powder, while only about 12.0% of CUR was dissolved for pristine microcrystal CUR and 5.9% for PM of buck CUR and excipients in the same conditions. There was an interesting finding that the release of CUR from the PM was delayed by 1 hour compared with that of the pristine group. It may be caused by the adhesiveness of TPGS, which was like a gel after swelling. Along with the dissolving of TPGS, the release of CUR from the PM began to surpass the pristine CUR due to the micelle effect but it was far worse from that of CUR-NS.

Stability of CUR-NS

The physical stability of the lyophilized CUR-NS powder was evaluated over 3 months at 4°C. During this storage period, the color and the reconstitution of the dried powder were unchanged. The particle size of the samples were consistent with the freshly prepared preparation, and the CUR content was not significantly changed, indicating that the lyophilized product has a shelf-life of at least 3 months at 4°C.

Pharmacokinetics and biodistribution of CUR-NS

CUR in biological matrix was determined based on the established method[41]. Chromatograms of CUR showed a stable baseline and good resolution between CUR and endogenous materials in plasma. The limit of quantification (LOQ) for CUR in biological sample was 0.015 μg/mL. The standard curves with CUR concentrations ranging from 0.015 to 1 μg/mL exhibited good linearity for all measured samples. The extraction recoveries of CUR in the concentrations of 0.015, 0.125 and 1 μg/mL from biological sample were more than 80%.

The pharmacokinetics of CUR-NS and CUR solution after i.v. administration in rabbits was described by a noncompartment model, and mean plasma profile of CUR was presented in Figure 9[42]. As shown in Figure 9, the mean residence time (MRT, 194.57 ± 32.18 minutes) for the CUR-NS formulation was considerably longer (11.2-fold) than that of CUR solution. The peak plasma concentration (C_{max}) of CUR-NS (25.54 ± 6.2 μg/mL) was significantly greater ($P < 0.01$) than that of CUR solution (8.17 ± 0.93 μg/mL). $AUC_{0-\infty}$ for CUR-NS (700.43 ± 281.53 μg/mL·min) was approximately 4.8-fold that of CUR solution (145.42 ± 9.29 μg/mL·min). The possible reason was that nanoparticles coated with hydrophilic polymer had a reduced opsonization and a longer period in circulation[43]. High mobility of linear poly (ethylene oxide) chains in TPGS might present to repel approaching proteins from the particle surface because the protein does not have sufficient contact time with the mobile chains[44], which delayed the residence time of CUR in blood. In our study, CUR plasma concentration could be still detected at 12 hours post injection of CUR-NS, but only up to 4 hours for CUR solution. Thus, CUR-NS could maintain a longer retention time in blood compared to CUR solution.

Similar to the result of pharmacokinetics, CUR concentration for CUR-NS was markedly higher than that of CUR solution in all tissues in mice at the tested time points as shown in Figure 10. It was interesting to find that the i.v. administration to mice of CUR solution resulted in a high concentration of CUR in lungs, with the level of CUR higher than 240 ng/g at 3 hours after dosing. However, the levels of CUR distributed into heart, liver, spleen, kidney, and brain were very low and only ranged from 20 to 100 ng/g. To our knowledge, this is the first study on the tissue distribution in vivo of the reported CUR solution with dimethyl acetamide and PEG 400 as mixed solvent, so further research is needed to explain the possible reason for the above results.

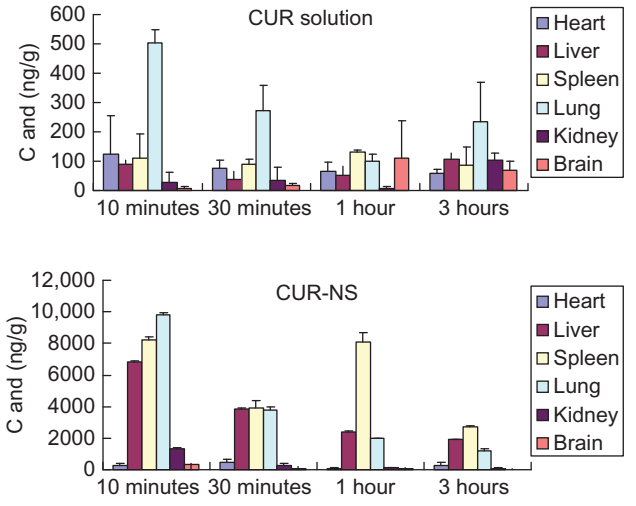

Figure 10. The concentrations of CUR in various tissues at different time following i.v. administration of CUR solution and CUR-NS in mice with the dose at 20 mg/kg (Data were given as mean ± SD, $n = 3$).

However, CUR-NS with an average size of 210.2 nm could be transported into the reticuloendothelial system such as liver, spleen, and lung via phagocytosis effect with the high concentration from 1000 to 10,000 ng/g. As shown in Figure 10, the concentrations in those tissues were many times (from 5 to 96 times) higher than that of the CUR solution. This may be the reason that contributed to the extension of the elimination time in plasma. CUR-NS, first taken up by RES, might dissolve slowly in the phagocytic cell and release slowly into blood circulation. On the contrary, lower viscosity of aqueous nanosuspension and higher permeation ability were the possible reasons contributing to the high concentrations of CUR in tissues. Similar results were reported by Zirar et al. for melarsoprol nanosuspension[45]. The aggregation of CUR in lung, spleen, and liver with high concentrations and long time presented great promise as an antioxidant and anticancer agent for the treatment of chronic obstructive pulmonary disease (COPD), Non-Hodgkin's lymphoma, alcoholic liver disease (ALD), and other tumors in those organs[46–48]. Moreover, the aqueous preparation, circumventing systemic exposure to the organic solvent, was more acceptable for injection, which may remarkably reduce side effects and thus have great clinical significance.

Conclusion

In this study, a new TPGS-stabilized intravenous injection nanocrystal suspension of CUR was produced by high-pressure homogenization. The obtained CUR-NS presented a sphere-like shape under TEM with mean particle size of 210.2 nm. The results of pharmacokinetic studies revealed a significant greater $AUC_{0-\infty}$ and prolonged MRT of CUR-NS compared to the reported CUR solution in rabbits after i.v. administration. Tissue distribution study in mice indicated that greater sequestration and higher CUR levels in the organs of the reticuloendothelial system were obtained for CUR-NS formulation compared with the CUR solution. The results showed that nanocrystal suspension represented a new and promising formulation for intravenous administration of curcumin.

Acknowledgments

This work is supported by a research grant (No.2008GG10002012) from Department of Shandong Science and technology, PR China.

Declaration of interest

The authors report no conflicts of interest. The authors alone are responsible for the content and writing of this paper.

References

1. Tong YQ, Wang Q, Hou HM. (2008). Protection by Chinese herbs against doxorubicin-induced focal and segmental glomerulosclerosis in rats. Drug Dev Ind Pharm, 34:663–7.
2. Xu PS, Van Kirk EA, Li SY, Murdoch WJ, Ren J, Hussain MD, et al. (2006). Highly stable core-surface-crosslinked nanoparticles as cisplatin carriers for cancer chemotherapy. Colloids Surf B Biointerfaces, 48:50–7.
3. Friedman MA, Woodcock J, Lumpkin MM, Shuren JE, Hass AE, Thompson LJ. (1999). The safety of newly approved medicines: Do recent market removals mean there is a problem? J Am Med Assoc, 281:1728–34.
4. Bava SV, Puliappadamba VT, Deepti A, Nair A, Karunagaran D, Anto RJ. (2005). Sensitization of taxol-induced apoptosis by curcumin involves down-regulation of nuclear factor-kappa B and the serine/threonine kinase Akt and is independent of tubulin polymerization. J Biol Chem, 280:6301–8.
5. Aggarwal BB, Surh YJ, Shishodia S. (2007). The molecular targets and therapeutic uses of curcumin in health and disease. Advances in experimental medicine and biology. New York: Springer.
6. Aggarwal BB, Harikumar KB. (2009). Potential therapeutic effects of curcumin, the anti-inflammatory agent, against neurodegenerative, cardiovascular, pulmonary, metabolic, autoimmune and neoplastic diseases. Int J Biochem Cell Biol, 41:40–59.
7. Anand P, Kunnumakkara AB, Newman RA, Aggarwal BB (2007). Bioavailability of curcumin: Problems and promises. Mol Pharm, 4:807–18.
8. Tonnesen HH, Masson M, Loftsson T. (2002). Studies of curcumin and curcuminoids. XXVII. Cyclodextrin complexation: Solubility, chemical and photochemical stability. Int J Pharm, 244:127–35.
9. Sigfridsson K, Lundqvist AJ, Strimfors M. (2009). Particle size reduction for improvement of oral absorption of the poorly soluble

drug UG558 in rats during early development. Dev Ind Pharm, 35:1479–86.
10. Lao CD, Ruffin MTT, Normolle D, Heath DD, Murray SI, Bailey JM, et al. (2006). Dose escalation of a curcuminoid formulation. BMC Complement Altern Med, 6:10–3.
11. Briones E, Colino CI, Lanao JM. (2008). Delivery systems to increase the selectivity of antibiotics in phagocytic cells. J Control Release, 125:210–27.
12. Keck CM, Müller RH. (2006). Drug nanocrystals of poorly soluble drugs produced by high pressure homogenisation. Eur J Pharm Biopharm, 62:3–16.
13. Basa S, Muniyappan T, Karatgi P, Prabhu R, Pillai R. (2008). Production and in vitro characterization of solid dosage form incorporating drug nanoparticles. Drug Dev Ind Pharm, 34:1209–18.
14. Li X, Gu L, Xu Y, Wang Y. (2009). Preparation of fenofibrate nanosuspension and study of its pharmacokinetic behavior in rats. Drug Dev Ind Pharm, 35:827–33.
15. Müller RH, Jacobs C, Kayser O. (2001). Nanosuspensions as particulate drug formulations in therapy. Rationale for development and what we can expect for the future. Adv Drug Deliv Rev, 47:3–19.
16. Ganta S, Paxton JW, Baguley BC, Garg S. (2009). Formulation and pharmacokinetic evaluation of an asulacrine nanocrystalline suspension for intravenous delivery. Int J Pharm, 367:179–86.
17. Peters K, Leitzke S, Diederichs JE, Borner K, Hahn H, Müller RH, et al. (2000). Preparation of a clofazimine nanosuspension for intravenous use and evaluation of its therapeutic efficacy in murine Mycobacterium avium infection. J Antimicrob Chemother, 45:77–83.
18. Van Eerdenbrugh B, Van den Mooter G, Augustijns P. (2008). Top-down production of drug nanocrystals: Nanosuspension stabilization, miniaturization and transformation into solid products. Int J Pharm, 364:64–75.
19. Gao L, Zhang DR, Chen MH, Duan CX, Dai WT, Jia LJ, et al. (2008a). Studies on pharmacokinetics and tissue distribution of oridonin nanosuspensions. Int J Pharm, 355:321–7.
20. Gao Y, Li LB, Zhai GX. (2008b). Preparation and characterization of pluronic/TPGS mixed micelles for solubilization camptothecin. Colloids Surf B Biointerfaces, 64:194–9.
21. Mu L, Seow PH. (2006). Application of TPGS in polymeric nanoparticulate drug delivery system. Colloids Surf B Biointerfaces, 47:90–7.
22. Feng SS, Mu L, Win KY, Huang GF. (2004). Nanoparticles of biodegradable polymers for clinical administration of paclitaxel. Curr Med Chem, 11:413–24.
23. Traber MG, Schiano TD, Steephen AC, Kayden HJ, Shike M. (1994). Efficacy of water-soluble vitamin E in the treatment of vitamin E malabsorption in short-bowel syndrome. Am J Clin Nutr, 59:1270–74.
24. Win KY, Feng SS. (2006). In vitro and in vivo studies on vitamin E TPGS-emulsified poly(d,l-lactic-/i co/-glycolic acid) nanoparticles for paclitaxel formulation. Biomaterials, 27:2285–91.
25. Bogman K, Erne-Brand F, Alsenz J, Drewe J. (2003). The role of surfactants in the reversal of active transport mediated by multidrug resistance proteins. J Pharm Sci, 92:1250–61.
26. Bogman K, Zysset Y, Degen L, Hopfgartner G, Gutmann H, Alsenz J, et al. (2005). P-glycoprotein and surfactants: Effect on intestinal talinolol absorption. Clin Pharm Ther, 77:24–32.
27. Dintaman JM, Silverman JA. (1999). Inhibition of P-glycoprotein by D-alpha-tocopheryl polyethylene glycol 1000 succinate (TPGS). Pharm Res, 16:1550–6.
28. Rege BD, Kao JPY, Polli JE. (2002). Effects of nonionic surfactants on membrane transporters in Caco-2 cell monolayers. Eur J Pharm Sci, 16:237–46.
29. Zhang JQ, Liu J, Li YL, Jasti BR. (2007). Preparation and characterization of solid lipid nanoparticles containing silibinin. Drug Deliv, 15:381–7.
30. Zhang DR, Tan TW, Gao L, Zhao W, Wang P. (2007). Preparation of azithromycin nanosuspensions by high pressure homogenization and its physicochemical characteristics studies. Drug Dev Ind Pharm, 33:569–75.
31. Ma ZS, Shayeganpour A, Brocks DR, Lavasanifar A, Samuel J. (2007). High-performance liquid chromatography analysis of curcumin in rat plasma: Application to pharmacokinetics of polymeric micellar formulation of curcumin. Biomed Chromatogr, 21:546–52.
32. Gao L, Zhang DR, Chen MH, Zheng TT, Wang SM. (2007). Preparation and characterization of an oridonin nanosuspension for solubility and dissolution velocity enhancement. Drug Dev Ind Pharm, 33:1332–9.
33. Mauludin R, Müller RH, Keck CM. (2009). Kinetic solubility and dissolution velocity of rutin nanocrystals. Eur J Pharm Biopharm, 36:502–10.
34. Wei CM, Zhang R, Wang BJ, Yuan GY, Guo RC. (2008). Determination and pharmacokinetic study of norcantharidin in human serum by HPLC-MS/MS method. Biomed Chromatogr, 22:44–9.
35. Voorhees PW. (1985). The theory of Ostwald ripening. J Stat Phys, 38:232–52.
36. Jacobs C, Kayser O, Müller RH. (2000). Nanosuspensions as a new approach for the formulation for the poorly soluble drug tarazepide. Int J Pharm, 196:161–4.
37. Hemar Y, Horne DS. (1999). A diffusing wave spectroscopy study of the kinetics of Ostwald ripening in protein-stabilised oil/water emulsions. Colloids Surf B Biointerfaces, 12:239–46.
38. Mishra PR, Al Shaal L, Müller RH, Keck CM. (2009). Production and characterization of Hesperetin nanosuspensions for dermal delivery. Int J Pharm, 371:182–9.
39. Baert L, Van't Klooster G, Dries W, Francois M, Wouters A, Basstanie E, et al. (2009). Development of a long-acting injectable formulation with nanoparticles of rilpivirine (TMC278) for HIV treatment. Eur J Pharm Biopharm, 72:502–8.
40. Hanafy A, Spahn-Langguth H, Vergnault G, Grenier P, Grozdanis MT, Lenhardt T, et al. (2007). Pharmacokinetic evaluation of oral fenofibrate nanosuspensions and SLN in comparison to conventional suspensions of micronized drug. Adv Drug Deliv Rev, 59:419–26.
41. Pak Y, Patek R, Mayersohn M. (2003). Sensitive and rapid isocratic liquid chromatography method for the quantitation of curcumin in plasma. J Chromatogr B Analyt Technol Biomed Life Sci, 796:339–46.
42. Langguth P, Hanafy A, Frenzel D, Grenier P, Nhamias A, Ohlig T, et al. (2005). Nanosuspension formulations for low-soluble drugs: Pharmacokinetic evaluation using spironolactone as model compound. Drug Dev Ind Pharm, 31:319–29.
43. Yao J, Zhou JP, Ping QN, Lu Y, Chen L. (2008). Distribution of nobiletin chitosan-based microemulsions in brain following i.v. injection in mice. Int J Pharm, 352:256–62.
44. Stolnik S, Illum L, Davis SS. (1995). Long *circulating* microparticulate drug carriers. Adv Drug Deliv Rev, 16:195–214.
45. Ben Zirar S, Astier A, Muchow M, Gibaud S. (2008). Comparison of nanosuspensions and hydroxypropyl-beta-cyclodextrin complex of melarsoprol: Pharmacokinetics and tissue distribution in mice. Eur J Pharm Biopharm, 70:649–56.
46. Gururajan M, Dasu T, Shahidain S, Jennings CD, Robertson DA, Rangnekar VM, et al. (2007). Spleen tyrosine kinase (Syk), a novel target of curcumin, is required for B lymphoma growth. J Immunol, 178:111–21.
47. Moghaddam SJ, Barta P, Mirabolfathinejad SG, Ammar-Aouchiche Z, Torres Garza N, Vo TT, et al. (2009). Curcumin inhibits COPD-Like airway inflammation and lung cancer progression in mice. Carcinogenesis, 30:1949–56.
48. Samuhasaneeto S, Thong-Ngam D, Kulaputana O, Suyasunanont D, Klaikeaw N. (2009). Curcumin decreased oxidative stress, inhibited NF-kappaB activation, and improved liver pathology in ethanol-induced liver injury in rats. J Biomed Biotechnol, 2009:981963.